Angiogenesis (2019) 22:197–209
https://doi.org/10.1007/s10456-018-9650-5

ORIGINAL PAPER

Staphylococcus aureus alpha toxin activates Notch in vascular cells

Sonia L. Hernandez[1] · Mildred Nelson[1] · Georgia R. Sampedro[2] · Naina Bagrodia[1] · Ann M. Defnet[1] · Bianca Lec[1] · Jared Emolo[1] · Rebecca Kirschner[1] · Lydia Wu[1] · Henry Biermann[1] · Stephanie Shen[1] · Juliane Bubeck Wardenburg[2,3] · Jessica J. Kandel[1]

Received: 9 January 2018 / Accepted: 24 September 2018 / Published online: 15 October 2018

Abstract

Staphylococcus aureus infection is one of the leading causes of morbidity in hospitalized patients in the United States, an effect compounded by increasing antibiotic resistance. The secreted agent hemolysin alpha toxin (Hla) requires the receptor A Disintegrin And Metalloproteinase domain-containing protein 10 (ADAM10) to mediate its toxic effects. We hypothesized that these effects are in part regulated by Notch signaling, for which ADAM10 activation is essential. Notch proteins function in developmental and pathological angiogenesis via the modulation of key pathways in endothelial and perivascular cells. Thus, we hypothesized that Hla would activate Notch in vascular cells. Human umbilical vein endothelial cells were treated with recombinant Hla (rHla), Hla-H35L (genetically inactivated Hla), or Hank's solution (HBSS), and probed by different methods. Luciferase assays showed that Hla (0.01 μg/mL) increased Notch activation by 1.75 ± 0.5-fold as compared to HBSS controls ($p < 0.05$), whereas Hla-H35L had no effect. Immunocytochemistry and Western blotting confirmed these findings and revealed that ADAM10 and γ-secretase are required for Notch activation after inhibitor and siRNA assays. Retinal EC in mice engineered to express yellow fluorescent protein (YFP) upon Notch activation demonstrated significantly greater YFP intensity after Hla injection than controls. Aortic rings from Notch reporter mice embedded in matrix and incubated with rHla or Hla-H35L demonstrate increased Notch activation occurs at tip cells during sprouting. These mice also had higher skin YFP intensity and area of expression after subcutaneous inoculation of *S. aureus* expressing Hla than a strain lacking Hla in both EC and pericytes assessed by microscopy. Human liver displayed strikingly higher Notch expression in EC and pericytes during *S. aureus* infection by immunohistochemistry than tissues from uninfected patients. In sum, our results demonstrate that the *S. aureus* toxin Hla can potently activate Notch in vascular cells, an effect which may contribute to the pathobiology of infection with this microorganism.

Keywords Notch · *Staphylococcus aureus* · Alpha-toxin · HUVEC

Abbreviations

Hla	Alpha toxin
EC	Endothelial cell
HUVEC	Human umbilical endothelial cell
EDTA	Ethylenediaminetetraacetic acid
ADAM10	A disintegrin and metalloproteinase domain-containing protein-10

Introduction

Staphylococcus aureus is a major cause of morbidity globally, and in the United States it contributes significantly to both hospital admissions and in-hospital morbidity [1, 2]. The increasing incidence of antibiotic-resistant strains increases the urgency of understanding the mechanisms by which this infection exerts its toxic acute effects, as well as potential long-term impact on infected patients, especially those with comorbid conditions. The major virulent toxin secreted by *S. aureus* is α-hemolysin (Hla). A Disintegrin

Electronic supplementary material The online version of this article (https://doi.org/10.1007/s10456-018-9650-5) contains supplementary material, which is available to authorized users.

✉ Sonia L. Hernandez
soniah@uchicago.edu

[1] Section of Pediatric Surgery, Department of Surgery, The University of Chicago, Chicago, IL, USA

[2] Department of Microbiology, The University of Chicago, Chicago, IL, USA

[3] Department of Pediatrics, Washington University at St. Louis, St. Louis, MO, USA

And Metalloproteinase domain-containing protein-10 (ADAM10), which is involved in ectodomain shedding, is the eukaryotic receptor for Hla [3–5], and mediates vascular injury caused by Hla [6]. Almost all isolates of *S. aureus* express Hla, including methicillin-resistant strains [7]. Recently, Hla has been shown to mediate VE-cadherin degradation in endothelial cells (EC) via ADAM10, affecting permeability [6]. Importantly, the Notch1 and 2 receptors are known ADAM10 targets [8].

Notch proteins are highly evolutionarily conserved. In mammals, the Notch pathway comprises the Jagged and Delta-like ligands, and the receptors Notch1 through Notch4. Both ligands and receptors are membrane-bound: in order for activation to take place, the ligand and receptor must be expressed in adjacent cells. Notch ligands are cleaved at Site 1 (S1) and can be post-translationally modified by glycosyltransferases, such as Fringe. Upon ligand binding, the negatively controlled region of the receptor unfolds, allowing ADAM10 to cleave the receptor at Site 2 (S2) [8], followed by a γ-secretase cleavage at Site 3 (S3). These events release the Notch intracellular domain (ICD), which then translocates to the nucleus. The ICD binds to the CSL (C protein binding factor, CBF-1) or RBPj in mammals, displacing corepressors and recruiting coactivators. Finally, the ICD is ubiquitinated after being targeted by SEL-10/FBW7.

The sequence of events leading to nuclear localization of the ICD upon ligand activation is commonly referred to as the canonical Notch pathway. Ligand-independent activation of Notch has been described, using divalent cation chelators such as ethylenediaminetetraacetic acid (EDTA) in vitro [9]. EDTA treatment results in Notch activation in cells, with millimolar Ca^{2+} stabilizing this effect [9], demonstrating that Notch activation can occur in the absence of ligand(s).

While Notch4 is largely restricted in its expression to ECs [10], Notch1 is expressed in other cell types, particularly during development. Notch1-null mice die before 11.5 days of gestation, due to vascular remodeling and neuronal defects [11]. Although mice lacking both copies of Notch4 develop normally, $Notch1^{-/-}$ $Notch4^{-/-}$ embryos display a more severe phenotype than Notch1 null embryos, suggesting that Notch4 contributes to normal angiogenesis.

Despite in vitro evidence that Notch can be cleaved by ADAM17, ADAM17-knockout mice die between E17.5 and birth, after angiogenesis takes place; their phenotype mimics tumor necrosis factor (TNF) null mice [12]. In contrast, ADAM10-deficient mice die with a defective vascular phenotype strikingly similar to Notch1-null mice, also at E9.5, with reduced neuronal Hes5 expression [13–15]. Furthermore, Notch signaling regulates adult intestinal stem cells, and regulates cell fate decisions to control epithelial cell homeostasis [16]. Mice lacking ADAM10 in epithelial cells demonstrate an identical intestinal phenotype to mice subjected to Notch1 and Notch2 blockade, or genetic deletion of epithelial Notch1 and Notch2, with decreased crypt cell proliferation [17, 18], indicating that ADAM10 is essential for and mediates most if not all of Notch activation in vivo. Together with vascular endothelial growth factor A (VEGFA), the Notch pathway has been shown to critically regulate not only developmental but also pathological angiogenesis ([19–22]; reviewed in [23]).

Given the role of ADAM10 in Hla binding and consequent Notch signaling, we hypothesized that Hla exposure would result in vascular and particularly endothelial Notch activation in vitro and in vivo. Because Notch activation controls multiple crucial functions in angiogenesis, Hla intoxication could exert significant effects on the vasculature in diverse tissues. In addition, Notch function in vasculature is context-dependent, and therefore such effects might be further modulated by the site of infection and Hla localization in tissues. In these studies, we examined the effect of Hla treatment on vascular cells in vitro and in vivo, and in multiple tissues with unique vascular patterning in murine and human hosts.

Materials and methods

rHla and Hla-H35L were generated in the Bubeck-Wardenburg lab as previously described [5]. Human umbilical endothelial cells (HUVEC) were kindly provided by Dr. Kitajewski (University of Illinois Chicago), and were cultured on Type I gelatin-coated (Millipore) plates using EBM-2 with 2% FBS and bullet kit (Lonza). Dimethyl sulfoxide (DMSO), the ADAM10 inhibitor GI254023X, and γ-secretase inhibitor *N*-[*N*-(3,5-difluorophenacetyl)-L-alanyl]-*S*-phenylglycine *t*-butyl ester (DAPT) were commercially obtained (Sigma). 5 mM EDTA (Sigma) was dissolved in Hank's balanced salt solution (HBSS) (Hyclone), pH adjusted to 7.5, and filter-sterilized prior to use.

LDH assay

These assays were performed according to the manufacturer's instructions (Dojindo), with the following exceptions: 1×10^3 passage 6 (p6) HUVEC were plated on a collagen coated 96-well plate. 24 h later, the media was replaced with increasing concentrations of Hla or Hla-H35L, and the assay stopped 12–21 h later. Where GI254023X was used, the inhibitor was added the night prior to the reagent addition, and stopped 20–24 h later. Percentages shown are relative to lysis buffer.

Polymerase chain reaction (PCR)

For Notch expression, mRNA was extracted from non-stimulated, non-transfected p6 HUVEC. cDNA was obtained

using VERSO cDNA kit (Invitrogen) following the manufacturer's instructions. PCR for each fragment was performed with Superscript (Invitrogen) for 40 cycles on a Biorad thermocycler, ran on a 1.5% agarose gel and visualized on QuantityOne 4.6.3 software (Biorad). For ADAM10 knockdown, mRNA was extracted 48 h after siRNA transfection, reverse-transcribed with VERSO kit (Invitrogen). 100 ng of cDNA was run with Taqman primers and FastTaq on a QuantStudio3 (Applied Byosystems) following the manufacturer's instructions. Beta actin was used as a housekeeping gene. For primer sequences and catalog numbers, see Supplementary Table 2.

Antibodies

See Supplementary Methods, Table 1.

Luciferase assay

HUVEC up to passage 6 were cultured on a 96-well plate, transfected with a pGL3-11-CSL-luciferase reporter construct kindly provided by Dr. Kitajewski (UIC) [24] and Renilla plasmid (Promega) using Fugene (Promega). 24 h later, the cells were stimulated with Hla, Hla-H35L, or 5 mM EDTA in HBSS for 15 min, followed with fresh supplemented EBM-2 media for 8 h. Cells were washed with PBS, lysed with 1 × passive lysis buffer, and analyzed with Promega Dual Luciferase Reporter assay kit according to the manufacturer's instructions on a Glomax Luminometer (Promega).

SDS-PAGE and Western blot

Proteins were denatured in 2 × sample buffer (Biorad) with beta-mercaptoethanol (Sigma), separated in 8% acrylamide gels using 40% acrylamide, transferred onto nitrocellulose membranes (LI-COR), blocked with 5% milk (Biorad) overnight, incubated with primary antibodies overnight at 4 °C, followed by 30–45 min infrared secondary antibody incubation (see Supplementary Table 1), and infrared captured and analyzed on Odyssey or OdysseyFc (LI-COR) or analyzed using ImageJ.

siRNA assays

HUVEC on a Falcon culture slide was transiently transfected with siRNA (ON-TARGETplus, Dharmacon) against ADAM10 pool (L-004503-00-0005), control, GAPDH control pool (D-001830-10-05), non-targeting pool (D-001810-10-05) or left untreated following the manufacturer's instructions using a 20 nM concentration of ADAM10 and Darmafect4 (0.1 µL/100 µL antibiotic free media). HUVEC were stimulated with Hla, EDTA or Hla-H35L 48 or 96 h after transfection and interrogated using immunocytochemistry (ICC) or SDS-PAGE and Western blot as described above (30–45 min after stimulation). A simultaneous plate with identically treated cells was assayed 48 h after transfection via real-time PCR to confirm the ADAM10 mRNA levels were significantly reduced.

Immunocytochemistry

HUVEC (p5 or p6) were grown on culture slides (Falcon) stimulated in HBSS as described above, except the stimulation lasted 10 min. Supplemented EBM-2 media was used for the remainder of the study. Staining was performed on acetone-fixed cells. For inhibitor studies, HUVEC were incubated overnight with 12 µM DAPT or DMSO prior to stimulation as follows: DMSO, Hla with DMSO or Hla with 12 µM DAPT for 15 min followed by acetone fixation.

Confocal images were captured in a Marianas confocal microscope (Zeiss) at a ×40 magnification, capturing 3–6 µM stacks at 0.7–2 µM intervals using Slidebook6 (Intelligent Imaging Innovations) and ImageJ (NIH) for image projection and analysis. Image quantification was performed on ImageJ (NIH) using the mean and standard deviation of at least four images per group. The DAPI channel was used to select the nucleus area to be quantified; this mask applied to the cN1 channel, and only this area was quantified. A background reading of the cN1 channel was subtracted from the cN1, and the mean of the multiple stacks was used.

Flow cytometry

P5 or p6 HUVEC were incubated with anti-human ADAM10 PE for 45 min at 4°, washed and fixed in 1% PFA until assayed. 10,000 events were recorded. Representative results of three independent cultures assayed are shown. Flow cytometry for Notch1 and Notch4 was performed by fixing the cells with 1% paraformaldehyde followed by permeabilizing with methanol prior to incubation with primary antibody or isotype control, followed by Alexa fluor 488 anti-rabbit (Notch1). All assays were performed in a FACSAria II (BD) and analyzed using Flojo software.

All animal experiments were approved by The University of Chicago IACUC. CBF:H2B-Venus mice were purchased from The Jackson Laboratory (Maine) [25], and bred to produce heterozygotes, in order to ensure one copy of the transgene was expressed in each mouse analyzed.

Retinal angiogenesis

Littermate pups were injected subcutaneously once daily from p2 to p5 with 0.0025 µg rHla or Hla-H35L (dissolved in 4–8 µL PBS) or PBS, and retinas harvested on p6 using a dissecting microscope (Leica), fixed with 4%

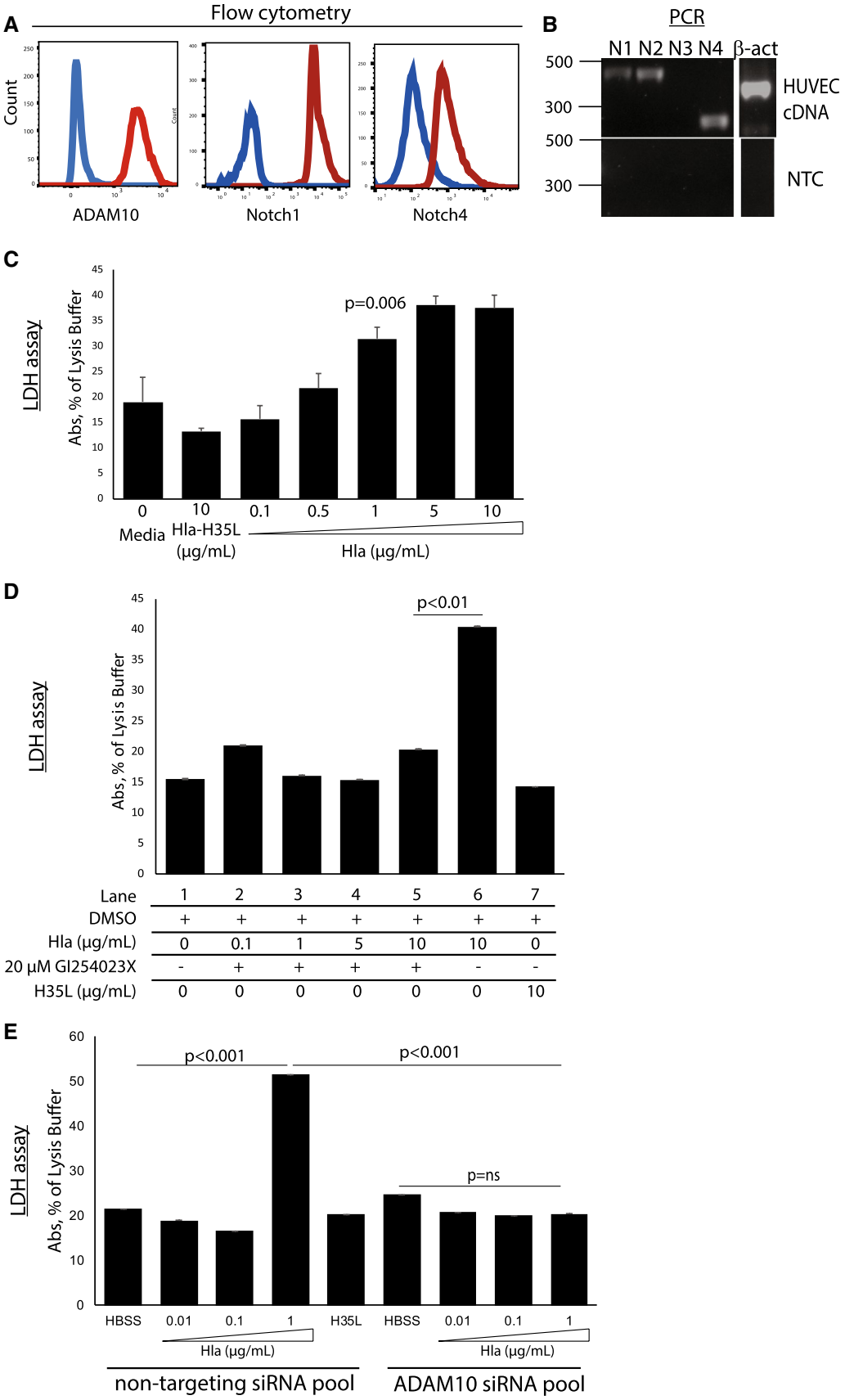
A
Flow cytometry
Count
ADAM10
Notch1
Notch4
B
PCR
N1 N2 N3 N4 β-act
500
300
500
300
HUVEC cDNA
NTC
C
LDH assay
Abs, % of Lysis Buffer
p=0.006
0 10 0.1 0.5 1 5 10
Media Hla-H35L (μg/mL)
Hla (μg/mL)
D
LDH assay
Abs, % of Lysis Buffer
p<0.01
Lane 1 2 3 4 5 6 7
DMSO + + + + + + +
Hla (μg/mL) 0 0.1 1 5 10 10 0
20 μM GI254023X - + + + + - -
H35L (μg/mL) 0 0 0 0 0 0 10
E
LDH assay
Abs, % of Lysis Buffer
p<0.001
p<0.001
p=ns
HBSS 0.01 0.1 1 H35L HBSS 0.01 0.1 1
Hla (μg/mL)
Hla (μg/mL)
non-targeting siRNA pool
ADAM10 siRNA pool

◂**Fig. 1** HUVEC are an appropriate model to study Hla-induced Notch activation in EC in vitro. **a** Over 99% of HUVEC express ADAM10 (left panel, red line) relative to unstained controls (blue) assessed by flow cytometry. HUVEC also express Notch1 and Notch4 by flow cytometry (middle and right panels), red line relative to isotype controls (blue). **b** PCR of HUVEC cDNA expressing Notch1, 2, and 4 (top panel), while no amplification was observed in no-template controls (NTC) (bottom panel). **c** Lactose dehydrogenase release indicates toxicity in vitro. LDH assays revealed significant toxicity starting at 1 µg/mL Hla or higher when compared to an untreated control ($p=0.006$); therefore, Hla is not lethal on HUVEC at the doses used in follow-up experiments (0.1 µg/mL) or lower. **d** ADAM10 is necessary for Hla toxicity in HUVEC: addition of 10 µg/mL Hla induces toxicity (lane 6), but the same concentration in the presence of GI254023X (lane 5) brings LDH levels to baseline (lane 1) and are not different to the genetically inactivated H35L levels (lane 7, $p=$ns). **e** While 1 µg/mL Hla increases LDH release relative to HBSS controls in non-targeting siRNA transfected HUVEC, this concentration does not induce LDH release in ADAM10 knockdown HUVEC (lane 4 vs. 9, $p<0.001$). Representative results of two experiments, with technical triplicates, p value represents t test. Graphs represent mean and standard deviation

PFA, permeabilized with 0.5% TritonX (Sigma), followed by IsolectinB4-647 (ThermoFisher) overnight incubation. Stained retinas were mounted with DAPI (Vector Labs) and imaged on a Marianas confocal microscope (Zeiss), images were acquired and deconvoluted on Slidebook, processed and quantified using ImageJ (NIH). 30 µM z-stacks at a 0.35 µM step were taken at ×40 magnification of at least five sections of the retina. Quantification of the Notch intensity in the endothelium was measured by selecting the endothelium on the lectin channel, transferring this area to the DAPI channel, allowing for the selection of the nuclei on the vasculature only. These were then selected using the threshold function, and this area was then measured in the Notch channel. Thus, we measured the Mean Intensity of (Notch) signal inside the Nuclei present in the vasculature (Lectin positive area). This analysis was performed for at least three layers per picture and the averages are shown as a single point in the graph.

Aortic ring assay

Aortas from six to eight 21-day-old Notch reporter mice were harvested as described by Baker et al. [26]. Briefly, 0.5-mm rings were incubated on Optimem overnight, followed by embedding in collagen matrix and cultured on Optimem with 25 ng/mL mVEGFA and 0.01 µg/mL rHla, H35L, or 0.01 µg/mL Hla with 20 µM GI254023X for 5 days, fixed in PFA, stained with the endothelial marker lectin, and imaged on a Marianas confocal microscope (Zeiss). Sprouts from four to eight aortic rings from each group, with maximum intensity projections of 30 µm thickness stacks, were processed on a Marianas confocal (Zeiss). Deconvoluted images were processed on ImageJ, and positivity scored visually on pictures. Non-parametric Mann–Whitney tests were performed on GraphPad software.

Staphylococcus aureus subcutaneous injection

6–8-week-old male Notch reporter mice received a single $1–4\times10^7$ 50 µL subcutaneous inoculation of *S. aureus* strains USA300/LAC (WT), or its isogenic ΔHla mutant (lacking Hla) as prepared as previously described [27], and their skin biopsies were analyzed 36 h, 8, and 16 days after inoculation. Eight to ten mice were inoculated per group per time point, and all were analyzed by Hematoxylin and Eosin. At least six were selected from each group and time point for further histological analysis. Tissues were fixed in 10% formalin or 4% PFA overnight, paraffin-embedded, and 5 µM sections analyzed by immunohistochemistry (IHC) as previously described [28]. Briefly, deparaffinized sections were incubated with rat anti-mouse endomucin (Santa Cruz Biotechnology) and anti-GFP (Cell Signaling), imaged on a LSM510 or Marianas confocal microscope (Zeiss), processed with LSM software (Zeiss) or Slidebook (Intelligent Imaging Innovations) followed by ImageJ (NIH) processing.

Patient tissues

Deidentified patient tissue slides from paraffin-embedded lungs and livers were obtained in accordance with IRB13-1225 from the University of Chicago Human Tissue Resource Center. IHC was performed as previously described [28].

Meta-analysis of three independent luciferase assay experiments (n = 5 per group) was performed using CMA software (Biostat Inc.). A comparison of two unmatched groups utilizing average means and SDs was performed. Assuming between-study homogeneity of the treatment effects, the results from three studies were analyzed with a fixed-effects model and summarized via p value and 95% CI. All figures were assembled in Adobe Illustrator (Acrobat). Significance values reflect $p<0.05$ or 0.005.

Results

HUVEC are an appropriate model to detect Hla activation of Notch in endothelial cells (EC)

Flow cytometry confirmed that ADAM10 is highly expressed in over 99% of HUVEC (Fig. 1a, left panel, red line vs. unstained control in blue). Consistent with published records [29], and given that HUVEC are primary cell isolates, we have confirmed expression of Notch1, Notch2, and Notch4 receptors in the HUVEC batches used in these experiments by non-quantitative PCR (Fig. 1b) and expression of

Notch1 and Notch4 by flow cytometry (Fig. 1b, middle and right panels red line vs. isotype control in blue).

In order to identify non-lethal concentrations of Hla on HUVEC in vitro, we incubated HUVEC with increasing concentrations of rHla (0.01–10 µg/mL) and measured lactose dehydrogenase (LDH) as a proxy for toxicity. We identified a significantly higher LDH release at 1 µg/mL or higher doses of Hla (Fig. 1c), and minor but detectable LDH levels at 0.5 µg/mL, while no LDH was detected at or under 0.1 µg/mL rHla was added (Fig. 1a, red arrow). As expected, HUVEC with media alone or high concentrations of the genetically inactivated Hla-H35L (10 µg/mL) generated no detectable levels of LDH (Fig. 1a). It is worth noting that, while no significant increase in LDH was detected at the 0.5 µg/mL concentration, we did observe morphological changes suggesting moderate toxicity. ADAM10 has been shown to mediate Hla toxicity [5], and we confirmed this in HUVEC by adding the ADAM10 inhibitor GI254023X to the highest tested Hla concentration (10 µg/mL, Fig. 1d, lane 5), which abrogates the LDH release from HUVEC incubated with the same concentration of Hla alone (Fig. 1d, lane 6). Finally, we knocked down ADAM10 (Supplementary Fig. 1) using an siRNA pool in HUVEC and incubated them with increasing Hla concentrations. Compared to non-targeting siRNA controls, ADAM10 knockdown protected HUVEC from lethality induced by 1 µg/mL Hla (Fig. 1e, $p < 0.01$). Quantitative PCR of ADAM10 indicates that ADAM10 siRNA reduced ADAM10 by more than 95% compared to untreated or non-targeting siRNA pools (Supplementary Fig. 1, $p = 0.0001$). Based on these results, we worked with concentrations of 0.1 µg/mL rHla or less for the remainder of these studies. In sum, HUVEC express ADAM10 and Notch proteins, and ADAM10 mediates Hla lethality indicating that this is an adequate in vitro model to evaluate Hla activation of Notch in EC.

Hla activates Notch1 in HUVEC

In order to detect Notch activation by immunoblotting and immunostaining, we used an antibody directed against the amino acid that is only exposed after S3 cleavage by γ-secretase, val1744, and will be referred to as cleaved Notch1 (cN1). This antibody will therefore only recognize the ICD after cleavage, will be approximately 110 kDa, and could be found in the cytoplasm or nucleus of the cell. EDTA has been shown to activate the Notch pathway in vitro via calcium chelation [9, 30]. We therefore used EDTA as a positive control in our in vitro experiments. In order to determine which concentration of Hla to test, we stimulated HUVEC with increasing concentrations of Hla, HBSS buffer, or EDTA for 10 min followed by a 30-min incubation time with full media. HUVEC demonstrate increased cN1 at a 0.001 and 0.01 µg/mL in concentration as revealed by immunoblotting, but not at the highest concentration tested of 0.1 µg/mL (Fig. 2a). HUVEC were incubated with HBSS, 0.01 µg/mL rHla, or EDTA for 10 min, followed by different periods of media incubation, and interrogated by SDS-PAGE and immunoblotting demonstrate that cleaved Notch1 (cN1) is already elevated relative to baseline and HBSS controls 15 min after stimulation (Fig. 2a). The highest levels of cN1 were observed between 30 and 45 min after stimulation with Hla, with this activation returning to baseline by 90 min after stimulation (Fig. 2b). We therefore selected 0.01 µg/mL rHla and an incubation time of 45 min after stimulation for the rest of the in vitro studies, except for Luciferase assays which required an 8-h incubation after stimulation.

Hla activates Notch in a specific manner

Luciferase assays confirmed that 0.01 rHla µg/mL increases Notch activation by 1.75 ± 0.5 fold compared to HBSS controls ($p < 0.05$), while EDTA caused a 5.4 ± 1.4 fold activation compared to HBSS ($p < 0.01$) (Fig. 3c). In comparison, the genetically inactivated Hla mutant protein (Hla-H35L) failed to activate Notch1 when analyzed via ICC, Luciferase assay, or Western blot (Fig. 3a–d), suggesting that ADAM10 is required for Hla-mediated Notch activation. Meta-analysis of three assays (n = 5 per group) shows that Hla-mediated Notch activation is significantly higher than HBSS (95% CI [0.15–1.86], $p = 0.021$), while H35L effects are not different from HBSS control (95% CI [−0.53 to 0.91], $p =$ ns).

ADAM10 and γ-secretase are necessary for Hla-induced Notch activation

In order to confirm whether Notch activation in response to Hla is mediated by ADAM10 and γ-secretase, we used the specific ADAM10 inhibitor GI254023X and the γ-secretase inhibitor DAPT. EDTA-dependent Notch activation is mediated by calcium, and can be blocked by γ-secretase and ADAM10 inhibitors [8].

Immunoblotting and immunostaining revealed that both GI254023X and DAPT abrogate cN1 upregulation resulting from Hla in HUVEC (Fig. 4a, lane 2 vs. 4 and Fig. 4a, lane 2 vs. 6, Fig. 4b, upper middle panel versus bottom left and middle panels, yellow arrows). The positive control EDTA increased cN1 levels (Fig. 4a, lane 7 and Fig. 4b upper right panel, white), while the genetically inactivated Hla-H35L did not change cN1 relative to DMSO vehicle (Fig. 4a, lane 8 and Fig. 4b, lower right panel). Quantification of this immunostain confirmed 1.93 ± 4.1 fold in nuclear cN1 increase after Hla relative to DMSO controls ($p = 0.01$). Incubating with DAPT or GI254025X prior to Hla brought nuclear cN1 levels back to baseline ($p =$ ns compared to DMSO controls) (Fig. 4c). Next, we knocked down ADAM10 levels by using siRNA pools. 48 h after

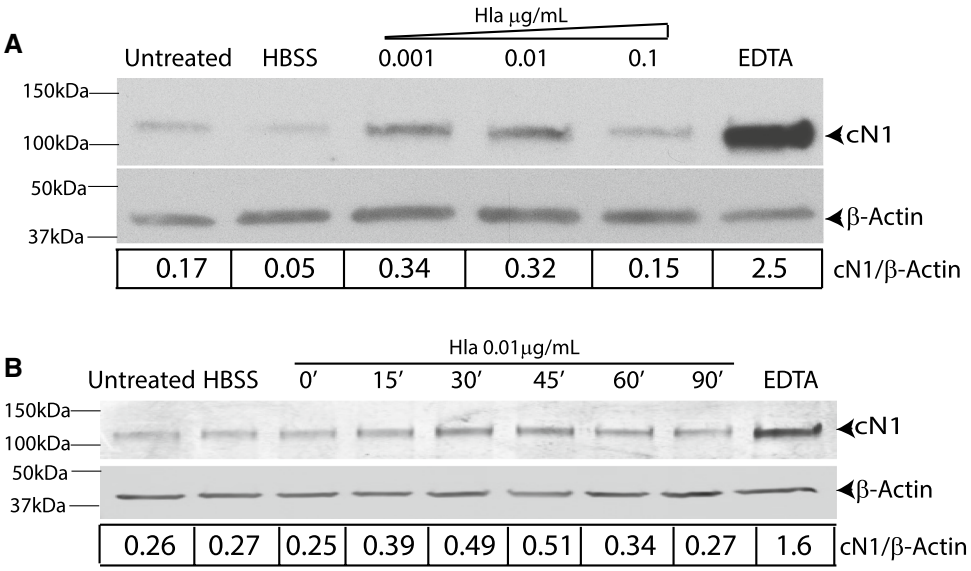

Fig. 2 rHla activates Notch1 in HUVEC, peaking between 30 and 45 min after Hla stimulation, at 0.01 µg/mL. **a** HUVEC were incubated with HBSS, increasing concentrations of rHla, or with 5 mM EDTA for 10 min, followed by media incubation for 45 min. Quantification of cN1 after SDS-PAGE and immunoblotting indicates cN1 is not altered by the highest rHla concentration tested (0.1 µg/mL), but increased when incubated at lower concentrations (0.01 or 0.001 µg/mL), approximately twofold relative to HBSS or Untreated controls. In contrast, the positive control EDTA increased cN1 by 15-fold relative to control levels. **b** HUVEC were treated with HBSS, 0.01 µg/mL Hla or 5 mM EDTA for 10 min followed by different time periods on media. cN1 levels started to increase 15 min after Hla was removed, peaks between 30 and 45 min, and then starts to decrease 60 min after Hla incubation, returning to comparable to untreated or HBSS levels after that. Hla elicited approximately twofold increase in cN1 levels compared to HBSS controls. The positive control EDTA measured 30 min after stimulation shows an approximately sixfold increase in cN1 levels compared to untreated or HBSS-stimulated controls. Representative results of three independent experiments. Relative values of cN1 to β-actin are shown under each lane

siRNA transfection, ADAM10 levels were decreased by more than 95% $p=0.0001$, (Supplementary Fig. 1) relative to untreated, non-targeting, and GAPDH siRNA transfected HUVEC (Supplementary Fig. 1). Next, we interrogated siRNA transfected HUVEC by ICC 96 h after transfection by stimulating as described in Fig. 3. In non-targeting siRNA HUVEC, similar to untreated cells, Hla increased cN1 levels compared to HBSS-treated controls (Fig. 4d, upper left panels, white insets). EDTA also increased cN1 levels, while Hla-H35L did not (Fig. 4d, upper right panels). In contrast, when ADAM10 levels were knocked down, both Hla and EDTA led to significantly decreased cN1 levels (Fig. 4d, lower panels, yellow arrow). Next, HUVEC were interrogated 48 h after siRNA transfection as described in Fig. 3, followed by SDS-PAGE and Western blot, confirming that ADAM10 knockdown failed to elicit a change in cleaved Notch1 compared to non-targeting control HUVEC (Fig. 4e, lanes 2 and 5). cN1 levels after EDTA stimulation, however, were not significantly decreased in the ADAM10 knockdown compared to non-targeting siRNA HUVEC when analyzed by immunoblotting (Fig. 4e). Although PCR analysis performed at this time revealed over 95% decrease in ADAM10 mRNA levels, ADAM10 protein levels at 48 h could still be present at high enough levels to be cleaved after EDTA stimulation. IHC performed at 96 h after siRNA transfection, however, did reveal a dramatic reduction in nuclear cN1 levels of ADAM10 knockouts stimulated with EDTA (Fig. 4d).

cN1 can be found in both cytoplasmic and nuclear localizations in both EDTA- and Hla-treated HUVEC. One example is shown at higher magnification in Supplementary Fig. 2, with white arrows pointing to the cN1 (red) in the nucleus (blue) of HUVEC, but not in the presence of ADAM10 inhibitor GI254023X.

In sum, 0.01 µg/mL rHla stimulations consistently revealed a twofold increase of cN1 in HUVEC relative to HBSS-stimulated, untreated control, or Hla-H35L levels, when assayed 30–45 min after stimulation and this activation is mediated by ADAM10 and γ-secretase.

Hla activates Notch in endothelial cells in vivo

In order to test whether Hla activates Notch in EC in vivo, we employed the retinal angiogenesis model. This model takes advantage of the well-characterized choreography of murine retinal blood vessel development, in which sprouts first grow in a two-dimensional plane originating from the optic nerve, and then move toward the periphery (vascular front) [31]. Venus mice are engineered to express a strong yellow fluorescent protein (YFP) signal localized to the nucleus as a result of Notch activation, which is readily colocalized by immunostaining for

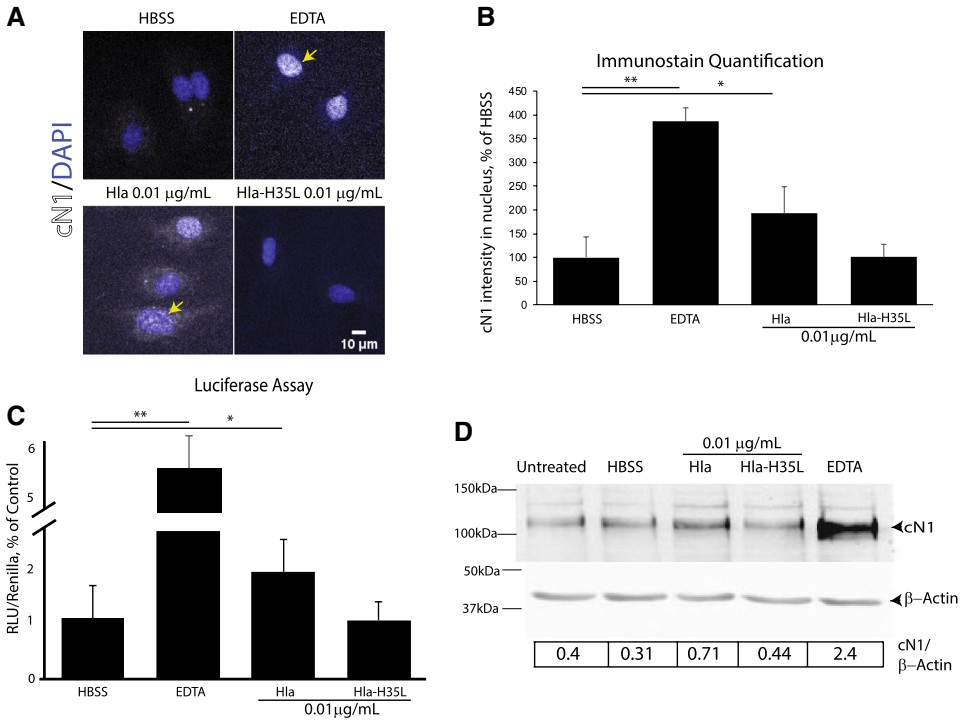

Fig. 3 Hla induction of cN1 in HUVEC is specific. **a** HUVEC stimulated with HBSS (control), 0.01 µg/mL rHla, 0.01 µg/mL genetically inactivated Hla-H35L, or EDTA for 10 min and then incubated with media for 45 min. EDTA and rHla induced nuclear cN1 (upper right panel, white, yellow arrows), while the Hla-H35L mutant form fails to elicit cN1 in HUVEC (bottom right panel). **b** cN1 Immunostain in DAPI-positive nuclei shown in (**a**) was quantified using ImageJ. Results indicate EDTA increased nuclear cN1 by fourfold relative to HBSS controls, while Hla induced a twofold increase. **c** Transfected HUVEC were stimulated for 15 min in the same conditions as in **a**, followed by 8 h of media incubation and luciferase assay. The Luciferase Notch reporter indicates that the positive control EDTA increases Notch activation by approximately 5.5-fold, whereas rHla stimulates Notch by almost twofold compared to HBSS controls; in contrast, Hla-H35L does not change Notch activation relative to controls. **d** HUVEC stimulated in equal conditions for 10 min followed by 45 min in media prior to SDS-PAGE. rHla led to a twofold cN1 increase compared to HBSS controls, whereas EDTA revealed an approximately sixfold increase. In comparison, the Hla-H35L construct had similar cN1 levels to HBSS. Representative results from three independent experiments are shown, *represents significance of 0.05, ** is less than 0.01; *p* values represent *t* test. Graphs represent mean and standard deviation

specific cell types. Venus littermates were injected with rHla daily from p2 to p5, followed by retina harvest at p6 and EC visualization with IsolectinB4, and mounted with DAPI. Representative images of YFP (activated Notch) in the nuclei of isolectin-positive area at the vascular bed are shown in Fig. 5a, the red arrows point at activated notch in lectin-positive areas. Quantification indicated that Notch activation is higher after Hla treatment than in H35L-treated controls (Fig. 5b, red arrows). Mean YFP intensity (green) in nuclei (blue) of ECs (white) was approximately 69% higher in rHla treated mice than in H35L littermate controls (Fig. 5b, $p < 0.0001$). These results were observed in two independent experiments, *p* value represents ANOVA.

Hla activates Notch in endothelial tip cells of aortic ring assay

Aortas from 3-week-old venus mice were used to perform an aortic ring assay, in which segments of the aorta were embedded in collagen matrix, and incubated for 5 days with 0.01 µg/mL rHla, 0.01 µg/mL H35L or 0.01 µg/mL Hla with 20 µM GI254023X, then fixed and labeled with the endothelial marker IsolectinB4 and imaged on a confocal microscope. Quantification of projections from 30 µM stacks reveal that, in contrast to H35L-incubated aortic rings in which only $14 \pm 15\%$ of sprouts display Notch activation in tip cells, more than $90 \pm 8\%$ of sprouts from aortic rings incubated with rHla displayed Notch activation in tip cells ($p < 0.0001$). In contrast, addition of the ADAM10 inhibitor completely suppressed Notch activation in tip cells induced by Hla completely (Fig. 5c, right panel), suggesting that ADAM10 mediates Notch activation in the tip cells of the aortic ring model. Representative images are shown in Fig. 5c; Lectin is pseudocolored white and Notch green, tip cells are indicated with a red arrow.

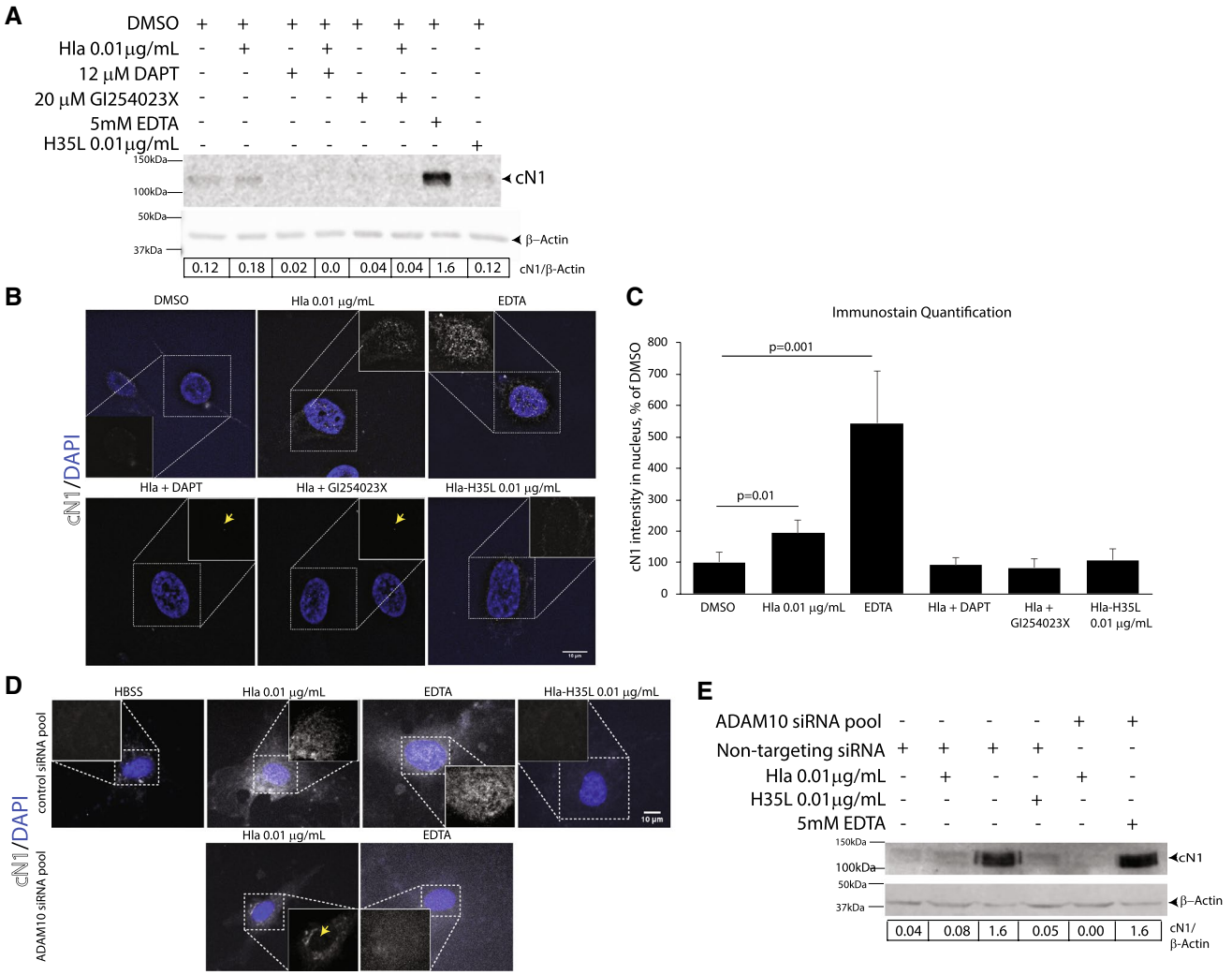

Fig. 4 ADAM10 and γ-secretase are necessary for Hla activation of Notch in HUVEC. **a** SDS-PAGE and immunoblot of HUVEC pre-incubated with DMSO, γ-secretase inhibitor (DAPT) or ADAM10 inhibitor (GI254023X), then stimulated with HBSS control, 0.01 μg/mL rHla, 0.01 μg/mL inactivated Hla-H35L, EDTA, or Hla with inhibitors for 10 min, followed by media for 45 min. Hla-induced cN1 levels (lane 2) were abrogated in the presence of DAPT and GI254023X (lanes 4 and 6). The EDTA-positive control increased cN1 levels relative to HBSS controls (lane 7). **b** HUVEC were pre-incubated with DMSO, DAPT or GI254023X, followed by DMSO, 0.01 μg/mL Hla or 0.01 μg/mL Hla with DAPT in HBSS for 15 min, fixed after 45 min. Hla increased cN1 (middle upper panel, white inset) compared to vehicle DMSO (upper left panel inset), and the EDTA-positive control increased cN1 as expected (upper right panel, inset). Both DAPT and GI254023X abrogated cN1 upregulation in response to Hla (Bottom left and middle panels; yellow arrows). Representative images of two independent experiments. **c** Quantification of (**b**) revealed a twofold increase in cN1 levels after Hla stimulation relative to HBSS controls which was reversed in the presence of DAPT and GI254023X. EDTA increased cN1 levels by 5.5-fold relative to DMSO. **d** HUVEC were transiently transfected with siRNA against ADAM10 or non-targeting, and 96 h later stimulated as described in Fig. 2a prior to fix and staining. Despite moderate toxicity, cN1 was upregulated by Hla and EDTA compared to HBSS in control transfected cells (top panels) and ADAM10 siRNA markedly reduced cN1 presence in both Hla (lower left panel, yellow arrow) and EDTA-treated cells (lower right panel). Cleaved Notch1 was pseudocolored white following Maximum Projection and No-neighbors deconvolution in Slidebook. **e** SDS-PAGE of HUVEC transfected and stimulated as in (**d**), and proteins were harvested after 48 h. ADAM10 knockdown prevented Hla induction of cN1 as observed in non-targeting siRNA HUVEC (lane 5 vs. lane 2). No difference was observed in EDTA stimulated HUVEC at 48 h. Representative blots of three independent experiments, *p* values represent t test. Graphs represent mean and standard deviation

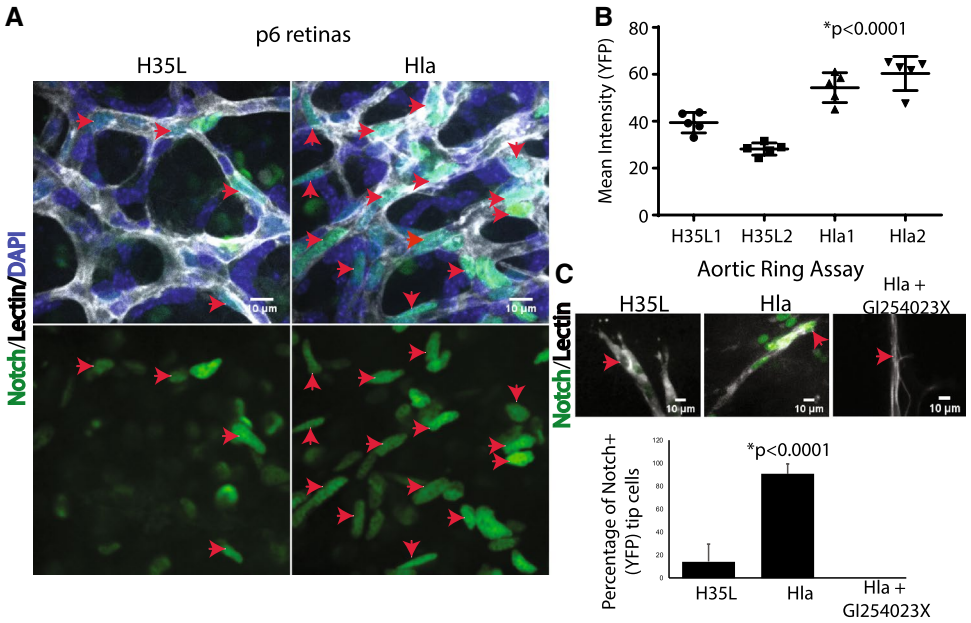

Fig. 5 Notch is upregulated in retinal EC of Notch reporter p6 pups treated with rHla, and in ex vivo aortic rings. **a** Littermate Notch reporter mice were injected daily with rHla subcutaneously from p2 to p5, and retinas harvested at p6 were stained with Isolectin B4 (white) and mounted with DAPI (blue). Confocal images of whole mounts were taken at a ×40 magnification, and mean YFP intensity (green) in areas overlapping Isolectin-B4 positive and DAPI positive areas (red arrows) were quantified using Image J. Representative images of 5–10 µM stacks are shown. Top panel shows overlay of lectin (white), Notch (green), and nuclei (blue). Bottom panels show Notch in that field (green), red arrowheads indicate activated Notch in nuclei of blood vessels is higher in Hla-treated pups (right panels). **b** Quantification of the mean grey intensity in the GFP channel (Notch) in DAPI positive nuclei revealed a 69% increase in Notch activity in Hla-treated mice compared to H35L controls. For quantification purposes, each layer of each picture was quantified separately and the average of those layers is shown. Representative results of two independent litters are shown. **c** Sprouts from aortic rings from Notch reporter mice incubated with 0.01 µg/mL H35L, Hla, or Hla with GI254023X for 5 days and stained for the endothelial marker lectin (white) resulted in tip cells with activated Notch signal (middle panel, green, yellow arrow), but not in aortic rings incubated with H35L (left panel). Addition of the ADAM10 inhibitor GI254023X eliminated all Notch signal from the sprouts (right panel). Eight aortic rings per group with six to ten sprouts per bead were counted and the percentage of positive tips per aortic ring is shown. Mann–Whitney test indicates a p value of <0.0001. Representative results of two independent experiments. Maximum projections from 30-µM-thick stacks are shown. Graphs represent mean and standard deviation

Staphylococcus aureus-derived Hla activates Notch in endothelial cells in a subcutaneous infection model

Finally, we asked whether Notch activation of EC occurs in the presence of actual *S. aureus* infection. In order to test this, we used a well-described skin infection model, injecting *S. aureus* secreting either WT Hla or no Hla (ΔHla) in adult male venus mice subcutaneously. Preliminary experiments indicated that Notch activation was detectable 36 h after infection and continued 8, and 16 days after infection (data not shown). Thus, we harvested and analyzed skin biopsies from ΔHla and WT Hla *S. aureus* infection 36 h, 8, and 16 days after inoculation. We observed an increase of YFP intensity and YFP-positive area in the skin adjacent to the presence of *S. aureus*, starting at 36 h after infection (Fig. 6a, white arrows). Quantification of fluorescence revealed a significant increase in the WT-infected group relative to ΔHla ($4.2\times10^{-5}\pm1.8\times10^{-5}$ vs. $7.9\times10^{-4}\pm6\times10^{-4}$ mean intensity relative to DAPI area, $p=0.008$ and $6.7\times10^{-6}\pm3.1\times10^{-6}$ vs. $7.7\times10^{-5}\pm6\times10^{5}$ YFP area/DAPI area, $p=0.002$) (Fig. 6b, c). On days 8 and 16 after inoculation, a striking Notch signal (green) was observed in the EC marker endomucin-positive cells in the WT group, but not in the ΔHla group (Fig. 6d). We also observed strong Notch activation (green) in the α-SMA-positive (red) vascular pericytes (Supplementary Fig. 3B, right panel). It is worth while noting that the vasculature in the Hla group was morphologically different, such as blood vessels having a larger lumen as depicted in Fig. 6d. Finally, we observed pronounced Notch activation in non-vascular cells, such as hair follicle cells, in the skin of the WT *S. aureus* group and not ΔHla, particularly 36 h after infection (data not shown). Together, these data suggest that Hla derived from *S. aureus* strongly activates Notch in vivo, in both vascular cells (endothelial and pericytes) and in other cell types.

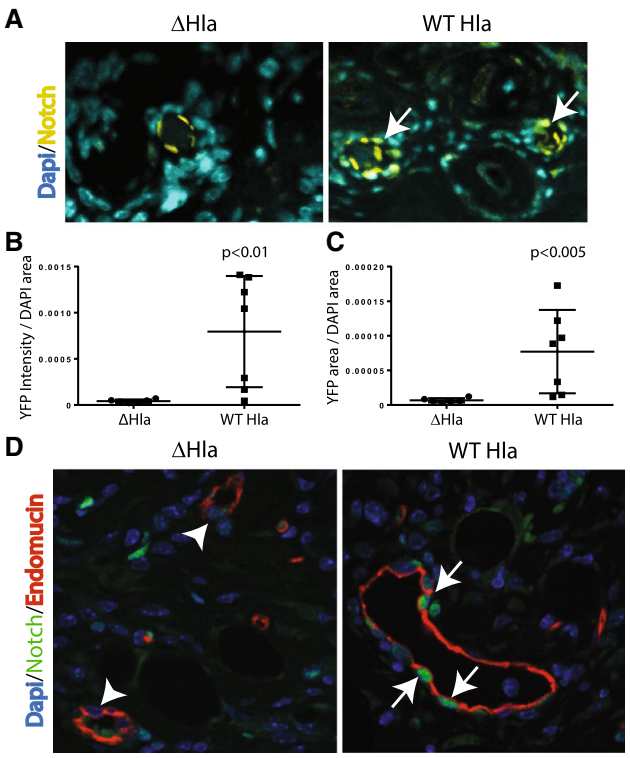

Fig. 6 *Staphylococcus aureus*-derived Hla toxin activates skin endothelial Notch activation. Notch reporter mice received subcutaneous *S. aureus* secreting Hla (WT Hla) or lacking Hla (ΔHla). **a** The epidermal and dermal layers adjacent to the infection site were analyzed 36 h after infection by histology, confocal images show increased Notch reporter (YFP) signal in skin infected with WT *S. aureus* compared to ΔHla. Representative images are shown. **b** Quantification of the YFP signal in the skin adjacent to the infection area shows a significantly higher YFP intensity/DAPI area ($p < 0.01$) and **c** a higher YFP area/DAPI area ($p < 0.005$). **d** IHC of skin 16 days after infection shows sustained Notch activation (left panel, arrows, green) in EC (red) of WT Hla skin compared to ΔHla strains with much lower Notch activation in EC (right panel, arrowheads, red). Graphs represent mean and standard deviation

Notch is activated in endothelial and vascular mural cells of human liver after *S. aureus* infection

Liver sections from a patient treated for culture-positive *S. aureus* sepsis show a dramatic upregulation of Notch in both EC (Fig. 7a, red, right panel, arrow) and vascular mural cells (Supplementary Fig. 3A, arrow) when compared to liver tissues of a patient without *S. aureus* infection (Fig. 7a, left panel). This upregulation was not observed, however, in lung tissues of the affected patient (data not shown), suggesting that Notch is selectively upregulated in a context-dependent manner in human hepatic EC and vascular mural cells as a result of systemic *S. aureus* infection.

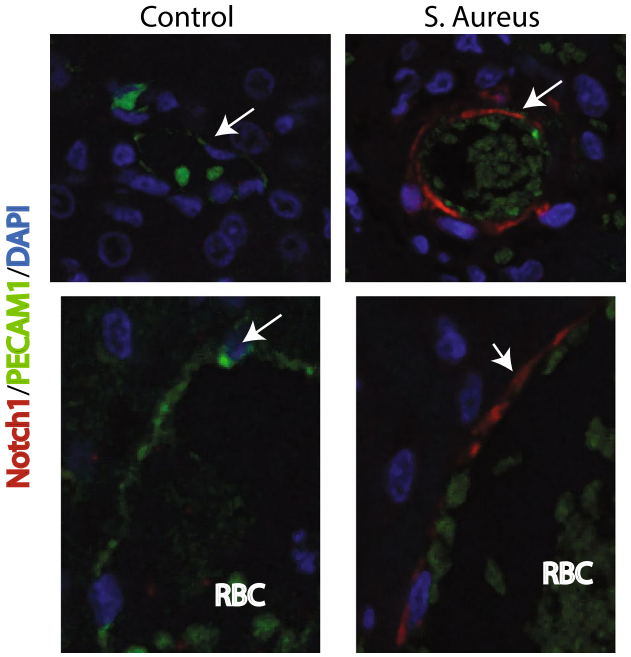

Fig. 7 Notch is increased in EC of human liver after *S. aureus* infection. Liver sections from a patient with *S. aureus* infection (right panels) had increased Notch expression (red) in PECAM-positive EC (green, white arrows), compared to a non-infected control (left panels). The red blood cells (RBC) indicate the vessel lumen

Discussion

Our results demonstrate that the *S. aureus* Hla toxin activates Notch in vascular cells, both in vitro and in vivo. In vitro, activation was detected at concentrations an order of magnitude lower than those causing lethality (between 0.01 and 0.001 µg/mL), peaking between 30 and 45 min after stimulation. Compared to the EDTA calcium chelator, Hla elicits a less pronounced but consistent Notch cleavage in vitro. The Hla mutant Hla-H35L does not elicit Notch activation, establishing that Hla multimer assembly and ADAM10 binding are required for Notch processing to take place.

The lack of Notch activation elicited by Hla in the presence of ADAM10 inhibitor GI254023X or the γ-secretase inhibitor DAPT suggests that canonical Notch receptor processing mediates Notch activation in response to Hla, and confirms the requirement of ADAM10 to mediate the effects of this toxin. These findings are supported by the reduced Notch activation after reduced ADAM10 levels via siRNA. If calcium flux mediated Notch activation, we would anticipate that progressively higher doses of Hla would cause increasing Notch signaling in EC. However, the highest concentration of Hla tested (0.1 µg/mL) did not activate Notch in HUVEC, and in fact we do not observe a dose–response curve in Notch activation, suggesting that calcium flux is not the mechanism by which Hla activates Notch in EC. Further testing of this

hypothesis is required, however, before calcium flux can be ruled out as a contributing mechanism. The lack of Notch activation elicited by Hla-H35L does indicate, however, that ADAM10 is required for Hla activation of Notch in HUVEC. Our immunostaining has revealed cN1's presence in both cytoplasm and nucleus of Hla treated HUVEC, consistent with canonical Notch signaling. The consequences of this activation, however, remain to be elucidated in future studies.

Notch stimulation found in the retinal angiogenesis model suggests that Hla activates Notch in EC in vivo. This conclusion is supported by the aortic ring assay findings, which indicate that Notch activation in cells at the tips of new sprouts could be a particular mechanism by which angiogenesis is subverted by a *S. aureus* infection via Hla secretion. Reversal of Notch activation in this model by the gamma-secretase and ADAM10 inhibitors as well as siRNA confirm that the canonical Notch pathway mediates this activation. Thus, this could represent a potential mechanism whereby *S. aureus* could modify neovascular patterning. Our understanding of the Notch pathway in angiogenesis indicates that Notch activity in stalk versus tip cells determines proliferation, the number of sprouts, the density and consequently the functionality of blood vessel networks. Therefore, the modification of Notch activation in tip cells could profoundly alter blood vessel sprouting by affecting tip versus stalk cell identity. The possibility of such an effect is highlighted in our observations of vascular Notch activation in the liver of a patient with staphylococcal septicemia, suggesting that these findings may be relevant to disease processes in humans.

The precise mechanism(s) by which Hla activates Notch in EC requires further study. In particular, the role of calcium flux in Hla-mediated Notch activation in EC remains unclear. Further, the downstream effects of Hla intoxication on angiogenesis in different tissues, in different physiologic states, and at different phases of development, remain incompletely defined. However, the widespread impact of deregulated Notch signaling and the increasing prevalence of *S. aureus* intoxication in human disease supports further investigation of these phenomena.

Acknowledgements We would like to thank Jan Kitajewski, Carrie Shawber, Henar Cuervo, and Darrell Yamashiro; The University of Chicago Imaging Core; The University of Chicago Human Tissue Resource Center; The University of Chicago Flow Cytometry Facility; Cancer Center Support Grant (P30CA014599). Funding for this project was provided by the Pediatric Cancer Foundation and The University of Chicago. This work was supported by NIH award AI097434 to J.B.W. G.R.S. has received support through NIH award 5 T32 GM7197 and the Genetics and Regulation Training Program at the University of Chicago.

Author contributions Conception and design: SLH, JJK, JB-W. Development of methodology: SLH, MN, GS, BL, RK. Acquisition of data: SLH, MN, GS, LW, BL, NB, AMD, JE, HB, RK, SS. Analysis and interpretation of data: SLH, MN, LW, BL, GS, NB, AMD, JE, JJK, RK, SS. Writing, review, and/or revision of the manuscript: SLH, JJK, JB-W. Administrative, technical, or material support: SLH, MN, LW, BL, NB, AMD, JE, RK, SS.

Compliance with ethical standards

Ethical approval All studies involving animals were in accordance with the ethical standards and approved by the IACUC at the University of Chicago. All procedures performed in studies involving human participants were in accordance with the ethical standards of the University of Chicago IRB and/or national research committee and with the 1964 Helsinki declaration and its later amendments or comparable ethical standards.

References

1. Le J et al (2017) Epidemiology and hospital readmission associated with complications of *Staphylococcus aureus* bacteremia in pediatrics over a 25-year period. Epidemiol Infect 145(12):2631–2639
2. Shenoy ES et al (2016) The impact of methicillin-resistant *Staphylococcus aureus* (MRSA) and vancomycin-resistant enterococcus (VRE) flags on hospital operations. Infect Control Hosp Epidemiol 37(7):782–790
3. Inoshima N, Wang Y, Bubeck J, Wardenburg (2012) Genetic requirement for ADAM10 in severe *Staphylococcus aureus* skin infection. J Invest Dermatol 132(5):1513–1516
4. Inoshima I et al (2011) A *Staphylococcus aureus* pore-forming toxin subverts the activity of ADAM10 to cause lethal infection in mice. Nat Med 17(10):1310–1314
5. Wilke GA, Bubeck J, Wardenburg (2010) Role of a disintegrin and metalloprotease 10 in *Staphylococcus aureus* alpha-hemolysin-mediated cellular injury. Proc Natl Acad Sci USA 107(30):13473–13478
6. Powers ME et al (2012) ADAM10 mediates vascular injury induced by *Staphylococcus aureus* alpha-hemolysin. J Infect Dis 206(3):352–356
7. Lozano C et al (2011) *Staphylococcus aureus* nasal carriage, virulence traits, antibiotic resistance mechanisms, and genetic lineages in healthy humans in Spain, with detection of CC398 and CC97 strains. Int J Med Microbiol 301(6):500–505
8. van Tetering G et al (2009) Metalloprotease ADAM10 is required for Notch1 site 2 cleavage. J Biol Chem 284(45):31018–31027
9. Rand MD et al (2000) Calcium depletion dissociates and activates heterodimeric notch receptors. Mol Cell Biol 20(5):1825–1835
10. Uyttendaele H et al (1996) Notch4/int-3, a mammary proto-oncogene, is an endothelial cell-specific mammalian Notch gene. Development 122(7):2251–2259
11. Al Haj Zen A, Madeddu P (2009) Notch signalling in ischaemia-induced angiogenesis. Biochem Soc Trans 37(Pt 6):1221–1227
12. Peschon JJ et al (1998) An essential role for ectodomain shedding in mammalian development. Science 282(5392):1281–1284
13. Krebs LT et al (2000) Notch signaling is essential for vascular morphogenesis in mice. Genes Dev 14(11):1343–1352
14. Swiatek PJ et al (1994) Notch1 is essential for postimplantation development in mice. Genes Dev 8(6):707–719
15. Hartmann D et al (2002) The disintegrin/metalloprotease ADAM 10 is essential for Notch signalling but not for alpha-secretase activity in fibroblasts. Hum Mol Genet 11(21):2615–2624
16. VanDussen KL et al (2012) Notch signaling modulates proliferation and differentiation of intestinal crypt base columnar stem cells. Development 139(3):488–497

17. Wu Y et al (2010) Therapeutic antibody targeting of individual Notch receptors. Nature 464(7291):1052–1057
18. Carulli AJ et al (2015) Notch receptor regulation of intestinal stem cell homeostasis and crypt regeneration. Dev Biol 402(1):98–108
19. Ridgway J et al (2006) Inhibition of Dll4 signalling inhibits tumour growth by deregulating angiogenesis. Nature 444(7122):1083–1087
20. Noguera-Troise I et al (2006) Blockade of Dll4 inhibits tumour growth by promoting non-productive angiogenesis. Nature 444(7122):1032–1037
21. Hellstrom M et al (2007) Dll4 signalling through Notch1 regulates formation of tip cells during angiogenesis. Nature 445(7129):776–780
22. Chigurupati S et al (2007) Involvement of notch signaling in wound healing. PLoS ONE 2(11):e1167
23. Thurston G, Kitajewski J (2008) VEGF and Delta-Notch: interacting signalling pathways in tumour angiogenesis. Br J Cancer 99(8):1204–1209
24. Kangsamaksin T et al (2015) NOTCH decoys that selectively block DLL/NOTCH or JAG/NOTCH disrupt angiogenesis by unique mechanisms to inhibit tumor growth. Cancer Discov 5(2):182–197
25. Nowotschin S et al (2013) A bright single-cell resolution live imaging reporter of Notch signaling in the mouse. BMC Dev Biol 13:15
26. Baker M et al (2011) Use of the mouse aortic ring assay to study angiogenesis. Nat Protoc 7(1):89–104
27. Becker RE et al (2014) Tissue-specific patterning of host innate immune responses by *Staphylococcus aureus* alpha-toxin. J Innate Immun 6(5):619–631
28. Banerjee D et al (2015) Notch suppresses angiogenesis and progression of hepatic metastases. Cancer Res 75(8):1592–1602
29. Murtomaki A et al (2014) Notch signaling functions in lymphatic valve formation. Development 141(12):2446–2451
30. Gupta-Rossi N et al (2001) Functional interaction between SEL-10, an F-box protein, and the nuclear form of activated Notch1 receptor. J Biol Chem 276(37):34371–34378
31. Stahl A et al (2010) The mouse retina as an angiogenesis model. Invest Ophthalmol Vis Sci 51(6):2813–2826